Magnetic behavior of superconducting and nonsuperconducting $RuSr_2Y_{2-x}Ce_xCu_2O_{10}$ ($x=0.5,1.0$)

I. Felner, I. Nowik, M. I. Tsindlickt, O. Yuli, I. Asulin, and O. Millo
The Racah Institute of Physics, The Hebrew University, Jerusalem 91904, Israel

V. P. S. Awana and H. Kishan
National Physical Laboratory, Dr. K.S. Krishnan Road, New Delhi 110012, India

S. Balamurugan and E. Takayama-Muromachi
Advanced Nano-materials Laboratory, National Institute for Material Science (NIMS), Tsukuba, Ibaraki 305-0044, Japan

(Received 2 July 2007; published 29 October 2007)

We report on magnetic, resistivity, Mössbauer spectroscopy, and scanning tunneling spectroscopy studies of ceramic superconducting (SC) and non-SC $RuSr_2Y_{1.5}Ce_{0.5}Cu_2O_{10-\delta}$ ($x=0.5$) and $RuSr_2YCeCu_2O_{10}$ ($x=1$). All materials studied were prepared at high oxygen pressure under the same conditions. Two magnetic transitions at T_{2M} and T_M ($T_{2M}<T_M$) are observed. For the SC $x=0.5$ material, both T_{2M} and T_M and saturation moments are *lower*, but its coercive fields are *higher* as compared to the non-SC $x=0.5$ sample material. In the $x=1$ sample, a dramatic increase in the magnetoresistance occurs at T_M.

DOI: 10.1103/PhysRevB.76.144514 PACS number(s): 74.70.Ad, 74.25.Ha, 75.70.Cn

I. INTRODUCTION

Much attention has been focused on a phase resembling the superconducting $RBa_2Cu_3O_7$ (RBCO, R=rare earth) materials, having the composition $\mathbf{M}Sr_2R_{2-x}Ce_xCu_2O_{10}$ (M-1222, **M**=Nb, Ru, or Ta, R=Eu and Gd).[1] The tetragonal M-1222 structure (space group $I4/mmm$) evolves from the $RBa_2Cu_3O_7$ structure by inserting a fluorite-type $R_{1.5}Ce_{0.5}O_2$ layer instead of the R layer in $RBa_2Cu_3O_7$, thus shifting alternate perovskite blocks by $(a+b)/2$. The **M** ions reside in the Cu (1) site and only one distinct Cu site [corresponding to Cu (2) in RBCO] with fivefold pyramidal coordination exists. Coexistence of weak ferromagnetism (W-FM) and superconductivity was discovered ten years ago in $RuSr_2R_{1.5}Ce_{0.5}Cu_2O_{10-\delta}$ (Ru-1222) layered cuprate systems,[2,3] and more recently[4] in $RuSr_2GdCu_2O_8$ (Ru-1212). In both systems, the superconducting (SC) state is due to the CuO_2 planes and the magnetic state, which coexists with the SC one, is confined to the Ru layers.

The SC state in Ru-1222 is well established and understandable, while the detailed magnetic structure of the Ru-O layers is still lacking. Bulk superconductivity is obtained below $T_C=32-50$ K, depending on the R/Ce ratio and on oxygen concentration.[5] The stoichiometric $RuSr_2RCeCu_2O_{10}$ ($x=1$) material, in which the oxygen concentration is 10, is magnetically ordered but is not SC. The decrease of the Ce content in $RuSr_2R_{2-x}Ce_xCu_2O_{10-\delta}$, affects the hole carrier concentration, thus changing the SC properties and the T_C values. Superconductivity occurs for Ce contents of 0.4–0.8 only.[5]

The most disputed question is the magnetic structure in Ru-1222. The $M(T)$ dc magnetic results exhibit two magnetic transitions, at T_{2M} (around 80–90 K) and at T_M (around 150–170 K) ($T_{2M}<T_M$). At low applied magnetic fields ($H<5-7$ kOe), irreversibility in the zero-field-cooled (ZFC) and field-cooled (FC) curves is observed up to T_{2M}. At $T_{2M}<T<T_M$, these two curves are very closed to each other and merge at T_M. In the isothermal $M(H)$ curves, relatively wide ferromagnetic (FM) hysteresis loops are opened up at low temperatures, with a coercive field H_C of ~450–700 Oe at 5 K. These loops become narrower as the temperature increases and practically close down at 70–80 K (below) T_{2M}. Above T_{2M}, small canted antiferromagnetic (AFM)-like hysteresis loops are reopened and the corresponding $H_C(T)$ curves show a peak with a maximum at around 125 K ($H_C \sim 150$ Oe) and become zero at T_M.[6] T_M is generally obtained directly from the temperature dependence of the saturation moment (M_{sat}). In spite of the unusual behavior of the $H_C(T)$ curves, the $M_{sat}(T)$ is a smooth curve which becomes zero at T_M. The accumulated results are compatible with two alternative scenarios discussed extensively in our previous publications.[7]

In contrast to the Ru-1212 system in which the antiferromagnetic nature of the Ru sublattice has been determined by powder neutron diffraction (NPD) studies,[8,9] the magnetic structure of Ru-1222 sample obtained from NPD is controversial. Mclaughlin *et al.* have related the extra peaks observed (for a non-SC material) below T_M to an AFM ordering of the Ru sublattice. From the magnetic peak intensities, they determined the Ru moments to be aligned along the c direction. The canting of Ru moments, which creates the W-FM nature discussed above, is not seen by their neutron diffraction studies. In addition to the Ru sublattice ordering, they concluded that at lower temperatures (which depend on the hole doping), the Cu spins order AFM in the a-b plane.[10] On the other hand, two NPD studies on Ru-1222 with ^{160}Gd as the R element failed to reveal any magnetic peaks, which are associated with the Ru sublattice below T_M.[11,12] Furthermore, ac susceptibility measurements on Ru-1222 materials demonstrated a sharp frequency dependence of the peak position at T_{2M}, which follows the Vogel-Fulscher law. This is typical character of the dynamics of spin-glass structure of interacting clusters,[13] which may explain why long-range magnetic order is not observed in NPD.

In attempting to understand the mechanism and the interrelations between the SC and the W-FM states in Ru-1222, an approach involving a comprehensive study of $RuSr_2Y_{2-x}Ce_xCu_2O_{10}$ (Ru-1222Y, $x=0.5$ and 1) materials is employed. Nonmagnetic Y^{3+} was used in order to diminish the paramagnetic contribution of Eu^{3+} and/or Gd^{3+} ions. This permits an easier direct interpretation of the intrinsic Ru magnetism. In contrast to the Ru-1222 (R=Eu and Gd) magnetosuperconductors, which are obtained at ambient pressure, the Y based materials can be synthesized only under high pressures. All Ru-1222Y samples published in the past were insulating non-SC materials down to 5 K. All attempts to induce superconductivity by annealing them under high oxygen pressure at elevated temperatures led to decomposition into a $RuSr_2YO_6$ (1216) phase.[6] We report here on $RuSr_2Y_{1.5}Ce_{0.5}Cu_2O_{10}$ which exhibits bulk superconductivity at $T_C=35$ K. The results obtained here will be compared to our published data on the non-SC $RuSr_2Y_{1.5}Ce_{0.5}Cu_2O_{10}$ sample.[6] This permits us to compare between two samples which have the same nominal composition ($x=0.5$), where one is SC and *magnetic* and the second is *magnetically ordered* only, thus enabling us to study the effect of the SC state on the magnetic features. It is proposed here that tiny differences in the amount of their oxygen concentration significantly alter their physical properties. In addition, we shall present data on $RuSr_2YCeCu_2O_{10}$ in which the oxygen content is supposed to be fixed.

II. EXPERIMENTAL DETAILS

Bulk samples of $RuSr_2Y_{2-x}Ce_xCu_2O_{10-\delta}$ ($x=0.5$ and 1) and 1% ^{57}Fe doped samples were prepared by the solid-state reaction technique. Prescribed amounts of RuO_2, SrO_2, $SrCuO_2$, $0.75Y_2O_3$, $0.5CeO_2$, 0.75CuO, and 0.25Cu (and ^{57}Fe) were mixed and pressed into pellets and heated at 1450 K for 3 h in 6 GPa of oxygen pressure.[14] Determination of the absolute oxygen content in these materials is difficult because CeO_2 is not completely reducible to a stoichiometric oxide when heated to high temperatures. ZFC and FC dc magnetic measurements at various applied field in the range of 5–300 K were performed in a commercial (Quantum Design) superconducting quantum interference device (SQUID) magnetometer. The in-phase component of the ac susceptibility (at $H_{dc}=0$ and amplitude of 50 mOe at various excitation frequencies) and the standard four contact magnetoresistance were measured by homemade probes inserted in the SQUID magnetometer. ^{57}Fe doped Mössbauer studies (MS) were performed at various temperatures by using a conventional constant acceleration drive and 50 mCi ^{57}Co:Rh source. The experimental spectra were analyzed in terms of several subspectra by a least squares fit procedure and the isomer shifts are relative to α-Fe measured at room temperature. Scanning tunneling spectroscopy data were acquired at 4.2 K. The $I(V)$ characteristics were measured along with the topographic images while momentarily disabling the feedback loop. Each measurement comprised at least three successive cycles to verify reproducibility and the absence of heating-hysteresis effects. The tunneling dI/dV vs V spectra (proportional to the local density of states) were obtained by numerical differentiation of the measured $I(V)$ curves.

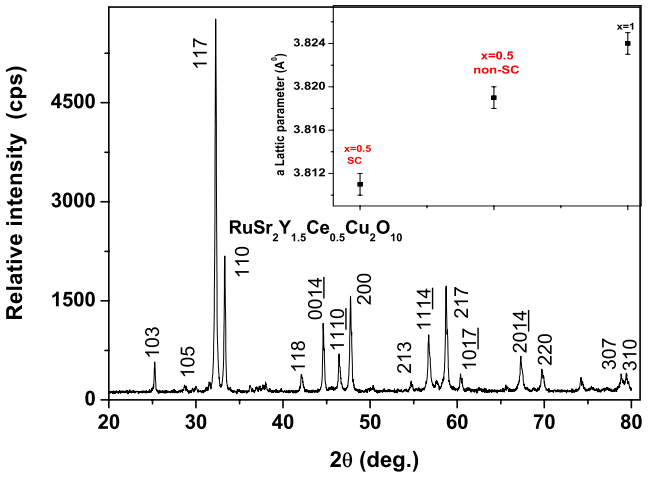

FIG. 1. (Color online) X-ray diffraction pattern of SC $RuSr_2Y_{1.5}Ce_{0.5}Cu_2O_{10}$. The a lattice parameters for the SC and non-SC $x=0.5$ and $x=1$ are shown in the inset.

III. EXPERIMENTAL RESULTS

The detailed crystal structure and the atomic positions in Ru-1222 were studied by synchrotron x-ray diffraction (XRD)[15] and NPD[11] experiments, which show that the RuO_6 octahedra are rotated $\sim 14°$ around the c axis and that this rotation is essentially the same for $x=1$ and $x=0.5$. There is no evidence for supercell peaks in the Ru-1222 samples. Figure 1 shows the XRD pattern of SC $RuSr_2Y_{1.5}Ce_{0.5}Cu_2O_{10}$ ($x=0.5$) sample at ambient temperature, which can be indexed on the basis of a body-centered tetragonal structure (space group $I4/mmm$) and yields the lattice parameters $a=3.810(1)$ Å and $c=28.43(1)$ Å. The lattice parameters for $RuSr_2YCeCu_2O_{10}$ ($x=1$) are $a=3.824(1)$ Å and $c=28.41(1)$ Å. Due to the similarity of the ionic radii of Y^{3+} (1.01 Å) and Ce^{4+} (1.04 Å) and within the instrumental accuracy, the c lattice parameters of all Ru-1222Y compounds studied here ($x=0.5$ and $x=1$) are practically the same. On the other hand, the lattice parameter a is sample dependent. Figure 1 (inset) exhibits the increase of the a lattice parameters for the non-SC $x=0.5$ (3.819 Å) material reported in Ref. 6 and that for the $x=1$ material. Both ($x=0.5$) samples have been synthesized under the same conditions, and the reason for the discrepancy in their a lattice parameters and as a result in their physical properties is puzzling. The single difference is that $SrCuO_2$ and SrO_2 were used as starting materials, instead of SrO_2 used for the non-SC sample.[6] Within the limit of uncertainty, the lattice parameters of the ^{57}Fe doped samples are similar to those of the undoped materials. For the sake of clarity, (i) we first present the data obtained for the SC $RuSr_2Y_{1.5}Ce_{0.5}Cu_2O_{10-\delta}$ sample and then compare its magnetic behavior with that of the non-SC $x=0.5$ sample. (ii) We present the magnetic properties of the non-SC **Ru**$YCeSr_2Cu_2O_{10}$ ($x=1$) material, in which the oxygen concentration is fixed.

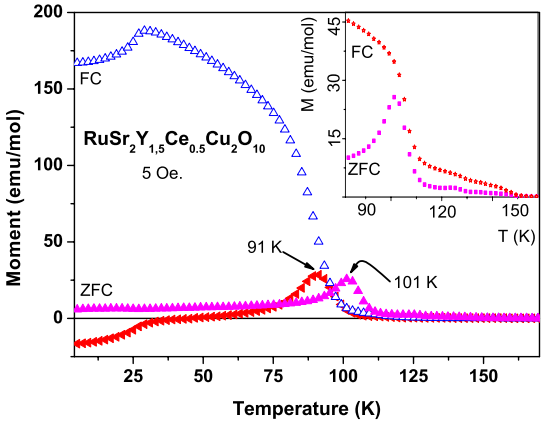

FIG. 2. (Color online) ZFC and FC susceptibility curves (measured at 5 Oe) for SC $RuSr_2Y_{1.5}Ce_{0.5}Cu_2O_{10}$ and the ZFC curve for the non-SC $x=0.5$ material. The inset shows the high temperature range of ZFC and FC plots for the non-SC sample. Note the peak in the ZFC branch at 125 K.

A. Superconducting and nonsuperconducting $RuSr_2Y_{1.5}Ce_{0.5}Cu_2O_{10}$ ($x=0.5$) materials

ZFC and FC magnetization (at $H_{ext}=5$ Oe) and the normalized ac susceptibility curves (at $H_{dc}=0$) for the SC and non-SC $x=0.5$ samples are shown in Figs. 2 and 3. For the SC material, a single peak at 91 K in both ZFC and ac plots is obtained and no second peak is observed at higher temperatures. The diamagnetic signal due to the shielding fraction (SF) dominates, and the net moment at low temperatures is negative. Moreover, in contrast to all other Ru-1222 SC materials, in the FC curve, the expected magnetic flux line expulsion in the SC state is clearly observed (Fig. 2). The W-FM component of Ru does not permit a quantitative determination of the SF. However, at low applied fields, the negative moment of the virgin $M(H)$ curve, increases linearly (up to 30 Oe), from which the deduced SF is ~25% of the $1/4\pi$ value, indicating bulk superconducting. For the non-SC Ru-1222Y material, the main peak shifts to 101 K, and a second peak is observed around 125 K. The ZFC and FC curves merge twice: at 105(2) K and at T_M(Ru) =152(1) K.

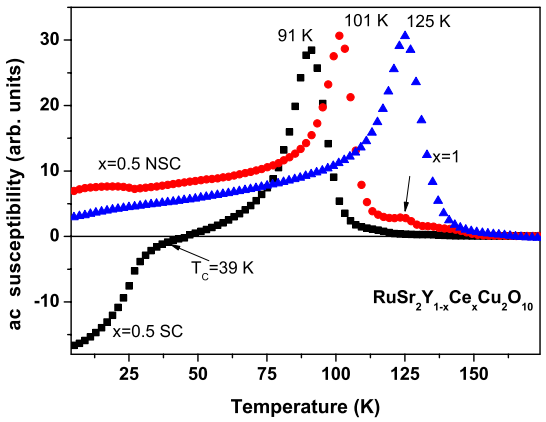

FIG. 3. (Color online) In-phase component of ac susceptibility curves for SC and non-SC $x=0.5$ materials and for the $x=1$ sample.

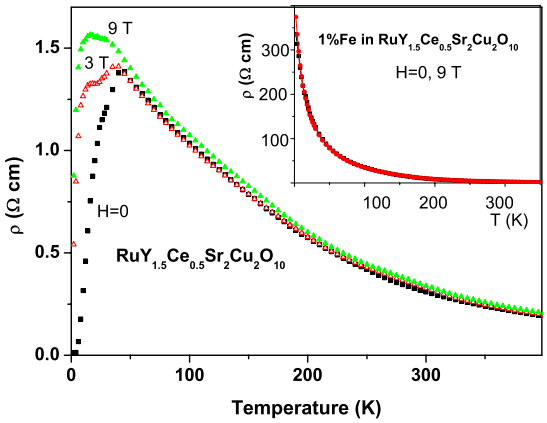

FIG. 4. (Color online) The temperature dependence of resistivity in magnetic fields up to 9 T for SC $RuSr_2Y_{1.5}Ce_{0.5}Cu_2O_{10}$ sample. The inset exhibits the resistivity for the Fe doped $x=0.5$ material at 0 and 9 T.

Figure 4 depicts the temperature dependence of resistivity for the SC sample measured at $H_{ext}=0$, 3, and 9 T, with SC onset at 40(1), 36(1), and 30(1) K, respectively. The high temperature resistivity (0.26 Ω cm at 300 K) increases slightly as the temperature decreases and no zero resistance is obtained down to 5 K. Note the slight difference between the $R(T)$ plot and the ac susceptibility curve in Fig. 3. This is in contrast to Ref. 16 in which the significant difference between the T_C values deduced from resistivity and magnetization data was attributed to the existence of the spontaneous vortex state in the SC state. The SC transitions (Fig. 4) are much broader than those observed in many other high temperature superconducting (HTSC) materials. Such a broadening is typical of underdoped Cu based high T_C materials, in which inhomogeniety in the oxygen concentration causes a distribution in the T_C values. Alternatively, one may argue for a phase separation of SC and non-SC phases, which coexist in the SC sample. However, the well-defined single sharp peaks in the ac curve (Fig. 3) rule out this option. For a two-phase material, two peaks should be seen in the ac plot.

The peak position in the ac curve for 1 at. % ^{57}Fe doped in $RuSr_2Y_{1.5}Ce_{0.5}Cu_2O_{10}$ sample is 90 K, but this material (which was prepared under similar conditions) is not SC down to 5 K and its $R(T)$ values are 2 orders of magnitude higher (Fig. 4, inset). This is in contrast to other Ru-1222 materials (and other HTSC systems as well), in which for 1% Fe, the SC state is retained but with a lower T_C. This suppression will be explained later. The magnetoresistance (MR), up to 9 T, properties of the two $x=0.5$ materials were studied extensively (not shown) and exhibit a behavior similar to that measured in other Ru-1222 systems.[10] For the Fe doped sample, MR (at 9 T) is about 4% at 50 and 100 K and only 0.6% above T_M, at 200 K.

As stated above, it was reported that in the non-SC Ru-1222Ysample (as well as in other Ru-1222 systems), the main peak position (T_f) in the ac susceptibility is frequency (f) dependent and shifts to higher temperatures with f.[13] It appears that the f versus $1/T_f$ plot is linear.[17] This trend

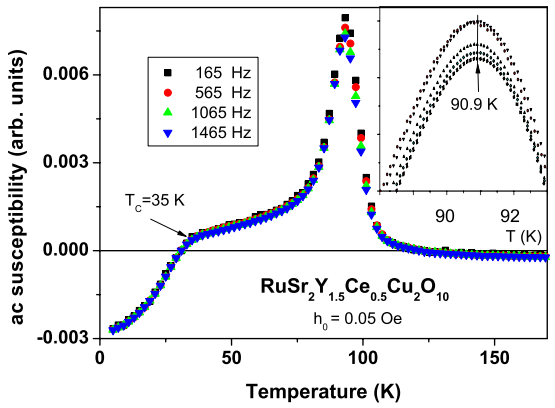

FIG. 5. (Color online) In-phase component of ac susceptibility of SC $RuSr_2Y_{1.5}Ce_{0.5}Cu_2O_{10}$ at various amplitudes.

provides a clear signature for the existence of a spin-glass (SG) state in Ru-1222Y. The SG behavior may explain the absence of long-range magnetic reflection in NPD studies as discussed. In contrary, Fig. 5 shows the real ac susceptibility curves measured under $h_{ac}=0.05$ Oe at various frequencies. The inset exhibits the extensive measurements around $T_f=90.9(1)$ K and within the uncertainty limit (0.1 K); no shift in T_f is observed. Thus, no SG features are detected in our SC Ru-1222Y material.

With the purpose of acquiring information about the magnetic properties of the SC and non-SC samples, $M(H)$ measurements at various temperatures have been carried out. The $M(H)$ curves below T_M are strongly dependent on the field up to 5–7 kOe, until a common slope is reached (Fig. 6, inset). $M(H)$ can be described as $M(H)=M_{sat}+\chi H$, where χH is the linear contribution to M and M_{sat} corresponds to the magnetic contribution of the Ru sublattice. Figure 6 presents the temperature dependence of M_{sat}, which becomes zero at T_M(Ru). It is readily observed that for the SC $x=0.5$ sample, both M_{sat} and T_M(Ru) values are *lower* than those for the non-SC $x=0.5$ one. The values obtained are M_{sat} (at 5 K)=0.42 and 0.63 μ_B/Ru and T_M(Ru)=140 and 170 K, for the SC and non-SC materials, respectively. [Note

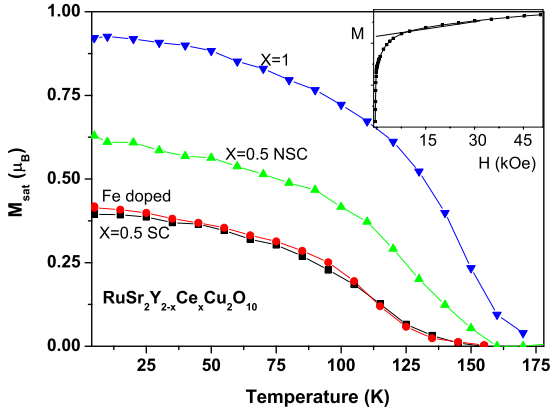

FIG. 6. (Color online) The temperature dependence of the saturation moment of Ru-1222Y samples. The inset shows a typical $M(H)$ curve measured below T_{2M}.

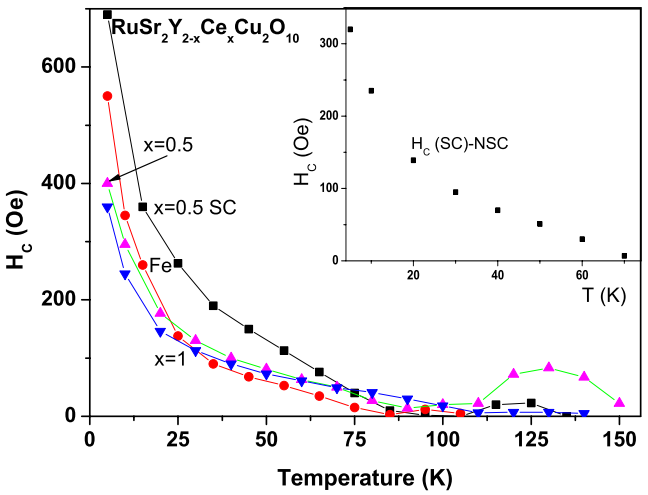

FIG. 7. (Color online) The temperature dependence of the coercive fields (H_C) of Ru-1222Y samples. The inset shows the difference between H_C of the SC and non-SC $x=0.5$ materials.

the similarity of the $M_{sat}(T)$ curves for the SC and the Fe doped materials.] These M_{sat} values are smaller than 1 μ_B, the expected moment for Ru^{5+} in the low-spin state ($g=2$ and $S=0.5$). This indicates that some canting on adjacent Ru spins occurs in the ordered state.

Another characteristic parameter obtained from the $M(H)$ measurements is the coercive field (H_C) deduced from hysteresis loops which are opened at low applied fields. The hysteresis loops can basically be divided into two regions. (1) Wide FM hysteresis loops are observed at low temperatures, which become narrower as the temperature increases and practically disappear below T_{2M} (Fig. 7). (2) For non-SC $RuSr_2Y_{1.5}Ce_{0.5}Cu_2O_{10}$, reappearance of the hysteresis loops is observed above T_{2M}, with a peak in $H_C(T)$ around 125 K, which is consistent with minor peak exhibited in Figs. 2 and 3. In contrast to the FM-like hysteresis loop obtained below T_{2M}, these loops exhibit an AFM-like feature.[6] The temperature dependence of H_C curves for Ru-1222Y is shown in Fig. 7. The $H_C(T)$ values of the SC material are *higher* than those of the non-SC samples (including the Fe doped sample). This determination can be easily observed in Fig. 8, which exhibits the low field region hysteresis loops at 5 K, for the two $x=0.5$ materials (note the small upturn at low applied fields due to the SC state). The H_C values obtained at 5 K are 690 and 550 Oe, for the SC and non-SC materials, respectively. Figure 7 (inset) depicts the difference between H_C values of the two materials as a function of temperature. In conclusion, the Ru-1222Y SC material has lower $M_{sat}(T)$ and T_M values but higher $H_C(T)$ values, as compared to the non-SC samples.

Similar behavior is observed in the Ru-1212 system, where the H_C values of the SC material are higher than those of the non-SC samples, regardless of whether superconductivity was suppressed by oxygen deficiency or by doping of La to the Gd site or to the Sr sites.[18] Thus, we tend to believe that the higher H_C values observed for all SC materials, in both Ru-1212 and Ru-1222 systems, are probably an experimental evidence for the presence of the spontaneous vortex state in the Ru magneto-SC materials.

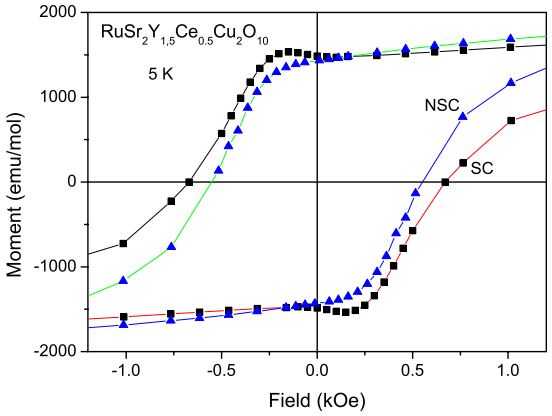

FIG. 8. (Color online) Hysteresis loops at 5 K for the two SC and non-SC $x=0.5$ materials.

In the paramagnetic range, the $\chi(T)$ curve follows the Curie-Weiss law and the net paramagnetic effective moment (P_{eff}) and Curie-Weiss temperature (θ) extracted are $P_{\text{eff}}=2.02(1)\mu_B$/Ru and $2.04(1)\mu_B$/Ru and $\theta=90$ and 136 K for the SC and non-SC samples, respectively. Similar P_{eff} values obtained for both $x=0.5$ materials exceed $1.73\mu_B$, the expected value for a localized Ru^{5+} low-spin state, but much smaller that the value obtained in Ref. 19.

Scanning tunneling microscopy (STM) and scanning tunneling spectroscopy measurements were performed at 4.2 K in order to measure the SC gap of SC material. Locally reproducible spectra showing very clear gap structures were acquired all over the sample (Fig. 9), where the gap values (as determined from fits to theory, see below) varied spatially between 7.6 and 8 meV (no correlation was found between the local topography and the gap value). We have checked that the measured gap structure did not depend on the STM setting, thus ruling out possible contributions of single-electron tunneling effects. Moreover, all I-V curves measured above T_C exhibited an Ohmic, gapless behavior, thus further corroborating that the gaps observed at 4.2 K are of SC origin. The tunneling spectra were fitted to the theory[20] of tunneling into a d-wave superconductor and using the Dynes

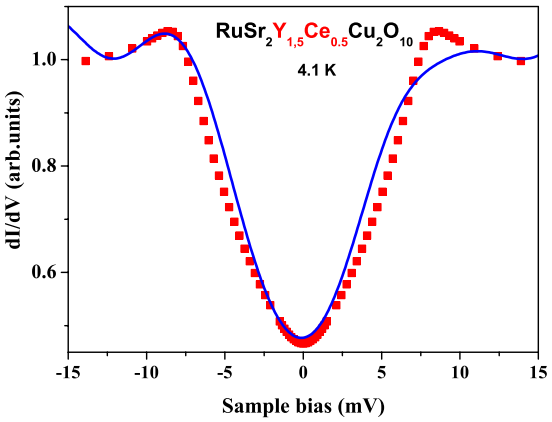

FIG. 9. (Color online) Normal differential conductance of the SC $RuSr_2Y_{1.5}Ce_{0.5}Cu_2O_{10}$ sample.

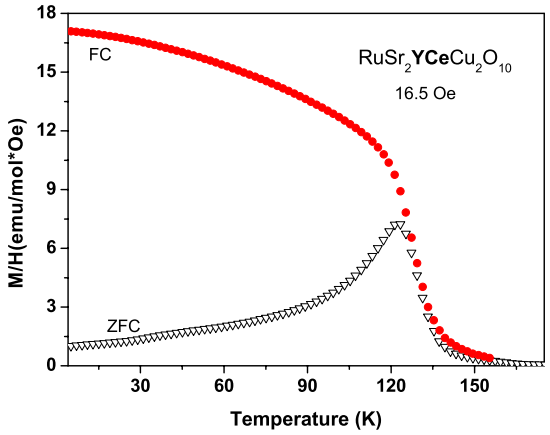

FIG. 10. (Color online) ZFC and FC susceptibility curves (measured at 16.5 Oe) for $RuSr_2YCeCu_2O_{10}$.

expression[21] for lifetime broadening of the quasiparticle density of states. Two fitting parameters were used: the SC gap parameter Δ and the lifetime broadening Γ. The best fits to our experimental data (all over the sample) yielded $\Delta=7.8(2)$ meV and $\Gamma=0.15(1)$ meV (e.g., Fig. 9, red dotted line). Such Δ values are in perfect agreement with the gap parameters found in other Ru-1222 system.[3] The calculated ratio $2\Delta(0)/k_BT_C\approx 5.6$ (k_B is the Boltzmann constant) is larger than the weak coupling BCS value for conventional s-wave superconductor, but typical for d-wave superconductors.[22] We note that the relatively low Γ obtained provides additional evidence for purity of the SC material.

B. $RuSr_2YCeCu_2O_{10}$ ($x=1$) sample and Mössbauer studies

It is well accepted that the $RuSr_2RCeCu_2O_{10}$ ($R^{3+}/Ce^{4+}=1$) sample serves as the parent stoichiometric insulator compounds (similar to La_2CuO_4). Since the valences of R^{3+}, Ce^{4+}, Ru^{5+}, Sr^{2+}, Cu^{2+}, and O^{2-} are conclusive, a straightforward valence counting yields a *fixed* oxygen concentration of 10. A central assumption is that the hole doping of the Cu-O planes, which results in metallic behavior and superconductivity in the $x<1$ materials, is obtained when Ce^{4+} ions are replaced by trivalent Y^{3+}. Reducing the Ce^{4+} content is partially compensated by depletion of oxygen; thus, the oxygen deficiency increases with R^{3+}.

The magnetic parameters for the $x=1$ material are as follows. The peak in ZFC branch (Fig. 10) at 125 K fits well with the ac data presented in Fig. 3, $T_M=175(3)$ K (deduced from Fig. 6) and $H_C(T)=360$ Oe (at 5 K). Note the similarity in the $H_C(T)$ curves of all the non-SC materials exhibited in Fig. 7. On the other hand, the M_{sat} (at 5 K) is $0.93\mu_B$/Ru (higher than for all $x=0.5$ materials) is very close to $1\mu_B$, the expected moment for Ru^{5+} in the low-spin state. The relatively high $M_{\text{sat}}(T)$ values (Fig. 6) are consistent with the high $P_{\text{eff}}=2.50(1)\mu_B$/Ru and $\theta=147$ K extracted from the Curie-Weiss like $M(T)$ curve in the paramagnetic range.

The typical semiconductinglike resistivity for the $x=1$ sample and the $MR_{9\ T}$ behavior are presented in Fig. 11. For

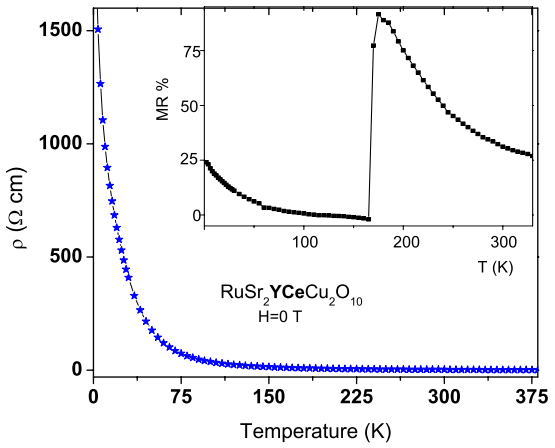

FIG. 11. (Color online) Resistance of $RuSr_2YCeCu_2O_{10}$ at $H=0$. The inset shows the temperature dependence of the MR for this sample (see text for definition).

the sake of clarity, $MR_{9\ T}$ is defined as $100^*[\rho(0)-\rho(9\ T)]/\rho(9\ T)$, where $\rho(0)$ and $\rho(9\ T)$ are the resistivities measured under $H=0$ and 9 T, respectively. Figure 11 shows an initial value of MR=25% which decreases monotonically up to T_M. This MR value is very close to the −MR=34% observed at 5 K in Ref. 10 for non-SC $RuSr_2Y_{0.2}Nd_{0.9}Ce_{0.9}Cu_2O_{10}$ in which the R^{3+}/Ce^{4+} ratio is close to 1. At $T_M=180$ K, $MR_{9\ T}$ increases dramatically up to 91%, which is the largest value reported for any Ru-1222 and any other copper oxide based systems at this strength fields. The large MR values in the Ru-1222 system are attributed to a strong spin-charge coupling within the CuO_2 planes.[10] The high MR values presented in Fig. 11 need more investigations and are comparable to those observed in the double-perovskite systems such as $Ca_xSr_{2-x}FeReO_6$.[23] This phenomenon (in the later system) was observed close to the magnetic transitions and is related to a coexistence of two crystallographic phases induced by the applied fields.

MS of dilute ^{57}Fe probes have proved to be a powerful tool in the determination of the magnetic nature of the probe's site location. When the Ru ions become magnetically ordered, they produce an exchange field on the Fe ions residing in this site. The ^{57}Fe nuclei experience magnetic hyperfine fields, leading to sextets in the observed MS spectra. MS spectra for 1 at. % ^{57}Fe doped in $RuSr_2YCeCu_2O_{10}$ measured at 300 and 90 K are presented in Fig. 12. MS have been performed also on the Fe doped $x=0.5$ material. The detailed analysis yields identical hyperfine parameters (within the limit of uncertainty) for both samples at each temperature. Therefore, the conclusions deduced from Fig. 12 are also valid to the $x=0.5$ doped material.

The bulk spectrum at 300 K contains two doublets: one of small and the other of large quadrupole splitting of equal intensities. In Ru-1222, the doped Fe ions may occupy either or both of Ru and Cu crystallographic sites. The small doublet [isomer shift (IS)=0.48 mm/s, $1/2e^2qQ=0.53(1)$ mm/s] and the large one [IS=0.26 mm/s, $1/2e^2qQ=0.89(1)$ mm/s] are attributed to Fe ions which occupy the Cu-O planes and Ru site, respectively.[3] In all other Fe doped Ru-1222 materials (and in Y-Ba-Cu-O systems as well), only a minor fraction of Fe (15%–20%) occupies the Cu-O planes and the rest reside in the Ru site. Since superconductivity is confined to the Cu-O planes, a few percent of doped Fe are needed to suppress superconductivity.[24] Unexpectedly, the analysis of the MS spectra at 300 K (Fig. 12) clearly shows that ~50% of Fe ions reside in the Cu-O planes. This relative fraction explains well the suppression of superconductivity by 1% Fe doped in $RuSr_2Y_{1.5}Ce_{0.5}Cu_2O_{10}$ presented above.

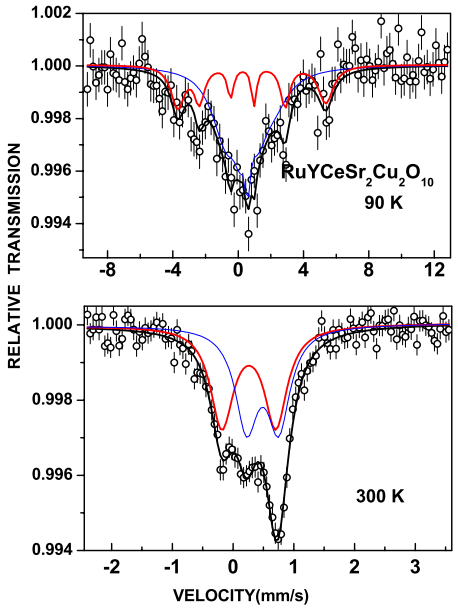

FIG. 12. (Color online) Mossbauer spectra of 1% Fe doped in $RuSr_2YCeCu_2O_{10}$ measured at 90 and 300 K.

As a final point of interest, we discuss the 90 K MS spectra shown in Fig. 12. It appears that the 300 K doublet corresponding to the Ru site is magnetically split into a sextet with an effective hyperfine field of $H_{eff}=280(3)$ kOe. The second doublet corresponding to the Cu site displays at 90 K a magnetically broadened (probably due to slow paramagnetic spin relaxation) subspectrum. These results exclude one of the scenarios raised later in Sec. IV. At 4.1 K, the two subspectra collapse into a broadened, effectively one sextet (not shown) with $H_{eff}=476(3)$ kOe, which means that the Fe ions that reside in the Cu sites also experience an induced magnetic field.

IV. DISCUSSION

NPD studies at 10, 60, and 160 K have been performed on the SC $RuSr_2Y_{1.5}Ce_{0.5}Cu_2O_{10}$ sample reported here.[27] W*eak* magnetic peaks were observed only at 60 and 10 K, indicating that they originate from the magnetic ordering of Ru spins below T_M(Ru). These additional magnetic peaks were fitted by an AFM magnetic structure of the Ru sublattice and the moments are aligned parallel to the c direction. The refined Ru magnetic moment is $1.5(3)\mu_B$, a value which is much higher than the M_{sat} values exhibited in Fig. 6. The magnetic reflections are weak and therefore the proposed AFM structure is not conclusive.[27] The NPD study failed to

determine the W-FM behavior below T_{2M}, the higher magnetic phase above T_{2M}, and the interplanar interactions between Ru spins.

One of the disputed questions in Ru-1222 materials is the origin the higher magnetic phase (above T_{2M}), whether it is intrinsic or not. This phase is more pronounced in the non-SC $RuSr_2Y_{1.5}Ce_{0.5}Cu_2O_{10}$ and exhibits peaks at 125 K in both ac and dc magnetic studies (Figs. 2 and 3). The accumulated results were interpreted in the past by two scenarios. Scenario (A), also supported by electron spin resonance studies,[25] assumes that the materials are *uniform as a whole* and that *all* the Ru ions behave in the same manner: At T_M, the Ru sublattice becomes AFM ordered as mentioned above, and at T_{M2} ($<T_M$), the whole material becomes W-FM ordered due to reorientation of the Ru moments, induced by the tilting of the RuO_6 octahedra from the crystallographic c axis.[11] At $T_C \sim 30$ K, the system as a whole becomes superconducting. Scenario (B) assumes a phase separation in that manner. Detailed MS analysis of ^{57}Fe and ^{119}Sn doped materials[7] as well as muon spin rotation studies[26] indicate with little doubt the occurrence of two magnetic phases, which order magnetically at two different temperatures. Due to inhomogeneity of the oxygen content across the samples, a *minority* fraction ($\sim 10\%$) starts to order magnetically at T_M, displaying hysteresis loops. When the temperature is lowered, the AFM alignment of the spins strengthens. H_C goes through a maximum, and then decreases and disappears. The *majority* fraction becomes W-FM ordered at T_{M2} and displays the typical FM-like hysteresis loops. The net canting moment depends on the R^{3+}/Ce^{4+} ratio, and this ratio obviously affects the oxygen concentration.

We measured here two samples with the same concentration, which were prepared at high pressure under similar conditions. Accidentally, it appears that one of them is SC and the second is not, which is probably caused by a tiny difference in their oxygen concentration. It is therefore assumed that the oxygen content in SC material is a bit higher than that of the non-SC $x=0.5$ sample. This allows us to compare between the magnetic properties of the two materials. The accumulated results obtained are as follows: (1) The T_M, T_{2M}, and the $M_{sat}(T)$ values are lower for the SC material (Figs. 2, 3, and 6). (2) On the other hand, its $H_C(T)$ values are higher. This may indicate the existence of the spontaneous vortex phase in the SC material (at least below T_C). (3) The second peak at 125 K is observable in the non-SC material only. (4) The absence of superconductivity in the Fe doped sample is due to unusual higher Fe fraction in the Cu-O planes. In this material, the second peak as well as the reappearance of the peak in H_C do not exist. (5) The magnetic sextet at 90 K for Fe ions residing in the Ru site (Fig. 12) is not connected to the second peak. It was argued that the minor sextets above T_{2M} are connected to the second peak observed in the dc and ac susceptibility curves. Since this sextet appears in a sample in which these peaks are absent, this scenario is excluded. (6) The $M_{sat}(T)$ curves (Fig. 6) decrease monotonically with temperature up to T_M, without any inflection points around T_{2M}, regardless of whether the sample is SC and whether the second peak exists. The dramatic increase of MR at T_M observed in Fig. 11 needs more consideration.

We may conclude with high confidence that all Ru-1222Y samples have basically the same magnetic structure (unknown at the present moment) and that all magnetic features observed in various materials, which differ in their oxygen content and/or distribution, are *intrinsic*. Further NPD studies of the interplanar interactions between Ru spins are necessary in order to fully elucidate the origin of the weak ferromagnetism observed in Ru-1222. We expect that this study will shed bright light on the complex magnetic structure of the Ru-1222 system.

ACKNOWLEDGMENTS

This research is supported in part by the Israel Science Foundation (ISF 2004 Grants Nos. 618/04 and 1565/04), by the Israeli Ministry of Science under the mutual India (DST)-Israel (MST) grant, and by the Klachky Foundation for Superconductivity. O.M. thanks the Harry de Jur chair for support. The NPL's authors thank their director, Vikram Kumar, for his kind interest in the present study.

[1] R. J. Cava, J. J. Krajewski, H. Takagi, H. W. Zandbergen, R. B. Van Dover, W. F. Peck, Jr., and B. Hessen, Physica C **191**, 237 (1992).

[2] I Felner, U. Asaf, Y. Levi, and O. Millo, Phys. Rev. B **55**, R3374 (1997).

[3] I. Felner, U. Asaf, Y. Levi, and O. Millo, Physica C **334**, 141 (2000).

[4] C. Bernhard, J. L. Tallon, Ch. Niedermayer, Th. Blasius, A. Golnik, B. Brucher, R. K. Kremer, D. R. Noakes, C. E. Stronach, and E. J. Ansaldo, Phys. Rev. B **59**, 14099 (1999).

[5] I Felner, U. Asaf, and E. Galstyan, Phys. Rev. B **66**, 024503 (2002).

[6] I. Felner, V. P. S. Awana, and E. Takayama-Muromachi, Phys. Rev. B **68**, 094508 (2003).

[7] I. Felner, E. Galstyan, R. H. Herber, and I. Nowik, Phys. Rev. B **70**, 094504 (2004).

[8] J. W. Lynn, B. Keimer, C. Ulrich, C. Bernhard, and J. L. Tallon., Phys. Rev. B **61**, R14964 (2000).

[9] J. D. Jorgensen, O. Chmaissem, H. Shaked, S. Short, P. W. Klamut, B. Dabrowski, and J. L. Tallon, Phys. Rev. B **63**, 054440 (2001).

[10] A. C. Mclaughlin, F. Sher, and J. P. Attfield, Nature (London) **436**, 829 (2005).

[11] C. S. Knee, B. D. Rainford, and M. T. Weller, J. Mater. Chem. **10**, 2445 (2000).

[12] J. W. Lynn, Y. Chen, Q. Huang, S. K. Goh, and G. V. M. Williams, Phys. Rev. B **76**, 014519 (2007).

[13] C. A. Cardoso, F. M. Araujo-Moreira, V. P. S. Awana, E.

Takayama-Muromachi, O. F. de Lima, H. Yamauchi, and M. Karppinen, Phys. Rev. B **67**, 020407(R) (2003).
[14] V. P. S. Awana and E. Takayama-Muromachii, Physica C **390**, 101 (2003).
[15] G. V. M. Williams and M. Ryan, Phys. Rev. B **64**, 094515 (2001).
[16] C. Y. Yang, B. C. Chang, H. C. Ku, and Y. Y. Hsu, Phys. Rev. B **72**, 174508 (2005).
[17] S. Garcia, L. Ghivelder, S. Soriano, and I. Felner, Eur. Phys. J. B **53**, 307 (2006).
[18] I. Felner and O. Ashkenazy, Physica C 460–462, 506 (2007).
[19] S. K. Goh, G. V. M. Williams, E. K. Hemery, and H. K. Lee, Phys. Rev. B **74**, 134506 (2006).
[20] Y. Tanaka and S. Kashiwaya, Phys. Rev. Lett. **74**, 3451 (1995).
[21] R. C. Dynes, V. Narayanamurti, and J. P. Garno, Phys. Rev. Lett. **41**, 1509 (1978).
[22] S. Kashiwaya, Y. Tanaka, M. Koyanagi, and K. Kajimura, Phys. Rev. B **53**, 2667 (1996).
[23] D. Serrate, J. M. De Teresa, P. A. Algarabel, J. Galibert, C. Ritter, J. Blasco, and M. R. Ibarra, Phys. Rev. B **75**, 165109 (2007).
[24] I. Felner, D. Hechel, A. Rykov, and B. Raveau, Phys. Rev. B **49**, 686 (1994).
[25] K. Yoshuda, H. Kojima, and H. Shimiza, J. Phys. Soc. Jpn. **72**, 3254 (2003).
[26] A. Shengelaya, R. Khasanov, D. G. Eschenko, I. Felner, U. Asaf, I. M. Savic, H. Keller, and K. A. MÜller, Phys. Rev. B **69**, 024517 (2004).
[27] A. C. Mclaughlin, I. Felner, and V. P. S. Awana (unpublished).